Annales Geophysicae (2003) 21: 1913–1929

Annales Geophysicae

Combining global and multi-scale features in a description of the solar wind-magnetosphere coupling

A. Y. Ukhorskiy[1], **M. I. Sitnov**[2], **A. S. Sharma**[2], **and K. Papadopoulos**[1,2]

[1]Department of Physics, University of Maryland at College Park, USA
[2]Department of Astronomy, University of Maryland at College Park, USA

Received: 5 November 2002 – Revised: 30 May 2003 – Accepted: 9 June 2003

Abstract. The solar wind-magnetosphere coupling during substorms exhibits dynamical features in a wide range of spatial and temporal scales. The goal of our work is to combine the global and multi-scale description of magnetospheric dynamics in a unified data-derived model. For this purpose we use deterministic methods of nonlinear dynamics, together with a probabilistic approach of statistical physics. In this paper we discuss the mathematical aspects of such a combined analysis. In particular we introduce a new method of embedding analysis based on the notion of a mean-field dimension. For a given level of averaging in the system the mean-filed dimension determines the minimum dimension of the embedding space in which the averaged dynamical system approximates the actual dynamics with the given accuracy. This new technique is first tested on a number of well-known autonomous and open dynamical systems with and without noise contamination. Then, the dimension analysis is carried out for the correlated solar wind-magnetosphere database using vB_S time series as the input and AL index as the output of the system. It is found that the minimum embedding dimension of $vB_S - AL$ time series is a function of the level of ensemble averaging and the specified accuracy of the method. To extract the global component from the observed time series the ensemble averaging is carried out over the range of scales populated by a high dimensional multi-scale constituent. The wider the range of scales which are smoothed away, the smaller the mean-field dimension of the system. The method also yields a probability density function in the reconstructed phase space which provides the basis for the probabilistic modeling of the multi-scale dynamical features, and is also used to visualize the global portion of the solar wind-magnetosphere coupling. The structure of its input-output phase portrait reveals the existence of two energy levels in the system with non-equilibrium dynamical features such as hysteresis which are typical for non-equilibrium phase transitions. Further improvements in space weather forecasting tools may be achieved by a combination of the dynamical description for the global component and a statistical approach for the multi-scale component.

Key words. Magnetospheric physics (solar wind–magnetosphere interactions; storms and substorms) – Space plasma physics (nonlinear phenomena)

Correspondence to: A. Y. Ukhorskiy (sasha@astro.umd.edu)

1 Introduction

The magnetospheric dynamics during substorms exhibits both globally coherent and multi-scale features. The globally coherent behavior of the magnetosphere is evident in such large-scale phenomena as the formation and ejection of plasmoids, the recovery of the field lines from the stretched to a more dipole-like configuration, the formation of global current systems, etc. At the same time, a number of small-scale phenomena observed during substorms, such as MHD turbulence, bursty bulk flows, current disruption, etc., are multi-scale in nature; viz. they have broad band power spectra in a wide range of spatial and temporal scales. The traditional approach of modeling the magnetospheric dynamics is the first principal approach which explicitly takes into account the nature of all forces in the system and then derives its collective behavior by considering interactions on the scales determined by the model. However, it is well recognized now that the collective behavior of a large number of complex many-body systems is determined by only generic dynamical features such as the range of interaction forces, dimensionality, and the nature of the order parameter. The dynamical models of such systems can be derived directly from data using general principals of nonlinear dynamics and statistical physics. The clear advantage of such data-derived models is their ability to reveal inherent features of dynamics, even in the presence of complexity and strong nonlinearity. Moreover, in many cases they still yield more accurate results and require much less computational power than the first principal models.

The earlier dynamical models of magnetospheric activity were motivated by the global coherence indicated by the geomagnetic indices and inspired by the concept of dynamical chaos. They were based on the assumption that the multi-scale spectra of observed time series are mainly attributed to the nonlinear dynamics of a few dominant degrees of freedom (see reviews: Sharma, 1995; Klimas et al., 1996). The dimension analyses of AE time series gave evidence of low effective dimension in the system (Vassiliadis et al., 1990; Sharma et al., 1993). Further elaboration of this hypothesis resulted in creating space weather forecasting tools based on local-linear filters (Price et al., 1994; Vassiliadis et al., 1995; Valdivia et al., 1996), data-derived analogues (Klimas et al., 1997; Horton et al., 1999), and neural networks (Hernandes et al., 1993; Gleisner and Lundstedt, 1997; Weigel et al., 2002). The low dimensional organized behavior of the magnetosphere on global scales is also evident in many in situ observations of the large-scale features of substorms by many spacecrafts including INTERBALL and GEOTAIL missions (Petrukovich et al., 1998; Nagai et al., 1998; Ieda et al., 1998).

However, the subsequent studies have shown that not all aspects of magnetospheric dynamics during substorms conform to the hypothesis of low dimensionality and thus cannot be accounted for within the framework of dynamical chaos and self-organization. For example, the power spectrum of AE index data (Tsurutani et al., 1990) and magnetic field fluctuations in the tail current sheet (Ohtani et al., 1995) have a power-law form typical for high dimensional colored noise. Prichard and Price (1992) have argued that by using a modified correlation integral (Theiler, 1991), a low correlation dimension cannot be found for the magnetospheric dynamics. Moreover, detailed analyses (Takalo et al., 1993, 1994) have shown that the qualitative properties of AE time series are much more similar to the bicolored noise than to the time series generated by a low dimensional chaotic system. It was also shown (Ukhorskiy et al., 2002a) that the low dimensional dynamical models leave out a significant portion of the observed time series which is associated with high dimensional multi-scale dynamical constituent.

One interpretation of these multi-scale aspects of magnetospheric dynamics was a multifractal behavior generated by intermittent turbulence (Borovsky et al., 1997; Consolini et al., 1996; Angelopoulos et al., 1999). Another approach to magnetosphere modeling is based on the concept of self-organized criticality (SOC). SOC was first introduced by Bak et al. (1987), who claimed that in "sand-pile" cellular automata the "criticality" (power distribution of avalanches which conduct the energy transport in the system) arises spontaneously without tuning of the control parameters. In SOC models the multi-scale features of substorms were reproduced by a "sand-pile" or other non-equilibrium cellular automata which explicitly take into account the large number of degrees of freedom in the system and the interactions among them on different scales (Consolini, 1997; Uritsky and Pudovkin, 1998; Watkins et al., 1999, 2001; Takalo et al., 1999; Chapman and Watkins, 2001; Uritsky et al., 2002). However, it was shown (Vespignani and Zapperi, 1998) that in order for the system to achieve criticality, the fine tuning of control parameters is required. In the cellular automata models, like "sand-pile" or "forest fire" models, the fine tuning corresponds to the vanishing values of input parameters. This makes these systems effectively autonomous and thus questions the relevance of the SOC framework to the magnetosphere, whose dynamics is, to a large extent, driven by the solar wind input. Moreover, original SOC models generally cannot account for the large-scale coherent features of the magnetosphere, since in most SOC models the multi-scale properties of the system are essentially independent of the global dynamics. To reconcile the multi-scale features with the global dynamics in a SOC-like model, the "sand-pile" model with the modified dynamical rules was proposed (Chapman, 2000; Chapman et al., 2001). In this model the scale-invariant avalanches were found to coexist with system-wide large-scale events. However, since such system-wide avalanches were found only in the "sand-pile" models with a vanishing rate of the energy input, this still cannot account for the specific global features of the actual magnetospheric dynamics. The SOC concept generalized for continuous systems (Lu, 1995) was further elaborated in the MHD model of the magnetospheric plasma sheet driven by a noise-like input (Klimas et al., 2000). However, the SOC regime in this model was achieved by assuming the specific form of the time dependence of the diffusion coefficient, whose relevance to the real magnetospheric plasma sheet is still an open question. On the other hand, it was also noted (Chang, 1999, 2000) that the properties of the criticality in SOC and in forced SOC models are very similar to those of the critical point in phase transitions.

In the physics of phase transitions, it is well known that the multi-scale behavior can naturally coexist with global dynamics. There are two different types of phase transitions which are intimately related to each other and coexist in a single system. The global dynamics of the system corresponds to the low dimensional manifold (coexistence surface) in the phase space of the system, which separates different phases of matter like the "pressure-temperature-density" surface in the case of a liquid-gas system. Due to the slow changes in the control parameters the state of the system evolves along the coexistence surface to the point where its stability is lost and it jumps to the state with lower energy through the first order phase transition. In first-order phase transitions one or more of the first derivatives of the appropriate thermodynamic potential (e.g. free energy) are discontinuous. The singular point of the coexistence surfaces where the order parameter (e.g. density in liquid-gas transitions, magnetization in ferromagnets) vanishes corresponds to the second order phase transitions and is called the critical point. At the critical point the first derivative of the thermodynamic potential is continuous while the second order derivative breaks. The approach to the critical point corresponds to an increase in fluctuations of the control parameter. At the critical point the fluctuations are scale-invariant and the correlation length (the size of the maximum fluctuation) diverges according to

the power law. It is worth noting that the fluctuation growth is not restricted only to the critical point vicinity. Indeed, the order parameter can exhibit fluctuations in a wide range of scales during the first order phase transitions as well, such as the growth of steam bubbles in boiling water. The more fundamental difference between the first and second order phase transitions is that during the former, the symmetry in the system is preserved, while during the later the symmetry breaks down (Stanley, 1971; Landau and Lifshitz, 1976). Phase transitions in natural, non-autonomous systems are essentially dynamic and non-equilibrium, resulting in additional properties such as hysteresis and dynamical critical exponents (Charkrabarti and Acharyya, 1999; Zeng et al., 1999; Hohenberg and Halperin, 1977).

The magnetospheric dynamics during substorms shares a number of properties with the dynamic non-equilibrium phase transitions (Sitnov et al., 2000; Sharma et al., 2001; Sitnov et al., 2001). In particular, using the global singular spectrum analysis of $vB_S - AL$ data Sitnov et al. (2000) have shown that the global magnetospheric dynamics is organized in a manner similar to the "pressure-temperature-density" diagram of the water-steam system. It was also suggested that the multi-scale properties of the data can be attributed to the dynamics in the critical point vicinity, i.e. second order phase transitions. Sitnov et al. (2001) also established the relation between the magnitude of the largest fluctuations of AL time derivative and the solar wind parameters similar to the input-output critical exponent β. The phase transition-like behavior was also found in other substorm signatures. In particular, it has been noted (Consolini and Lui, 1999) that the current disruption is similar to the second order phase transition. Consolini and Michelis (2001) proposed the cellular automation model of solar wind-magnetosphere coupling based on a revised forest-fire model (Drossel and Schwabl, 1992). The model has a repulsive fixed point similar to the critical point in phase transitions. The model was driven by the chaotic time series with the spectral properties of solar wind. It was found that the power spectrum of the integrated output has the broken power-law shape similar to the AE index spectrum and that the relaxation phenomena occurred as sporadic localized events similar to BBF.

The phase transition analogy clearly provides a framework for understanding the magnetospheric dynamics in which the global and multi-scale processes coexist. This also led to a new approach to the data-derived modeling of the solar wind-magnetosphere coupling that combines the methods of nonlinear dynamics and statistical physics (Ukhorskiy et al., 2002b). In the present paper we discuss the mathematical aspects of such a combined analysis. One of the central concepts of this analysis is the notion of mean-field dimension. For the given level of averaging in the system (the number of points in the phase space involved in the averaging) the mean-field dimension determines the minimum dimension of the embedding space in which the averaged dynamical system approximates the actual dynamics with the given accuracy (noise level). This also yields the distribution function in the reconstructed phase space which provides the basis for the probabilistic modeling of the multi-scale dynamical constituent. Previous analysis (Ukhorskiy et al., 2002a) has shown that dynamical models are very similar to the mean-field approach in phase transitions, since their outputs are obtained by averaging over the chosen range of scales in the reconstructed input-output phase space. Thus, the multi-scale features of the time series not captured by the low dimensional models are essentially the deviations of the data from the mean-field model. According to the phase transition analogy, the magnitudes of these fluctuations may be related to the solar wind input in a probabilistic fashion similar to the input-output critical exponent. The question is to what extent the magnetosphere can be described as a deterministic system and at what point the probabilistic consideration is necessary. In this paper we address this question with the use of the delay embedding analysis of a $vB_S - AL$ time series. We introduce a new technique of estimating the minimum embedding dimensions of input-output dynamical systems in the presence of a stochastic component.

It is now recognized that if all interaction scales are taken into account, the magnetosphere cannot be considered as a low dimensional system. However, introducing the probability density function on the attractor and performing the ensemble averaging in the embedding space leads to the smoothing of the small-scale high dimensional component. Such averaged system has a finite dimension and thus allows for a deterministic description. The dynamical model built into the embedding space of the averaged system yields the regular component of the observed time series. The portion of the time series not captured by the low dimensional model corresponds to the high dimensional constituent, which is smoothed away after the ensemble averaging and may be treated as noise from the dynamical modeling point of view. It is also found that the delay embedding of the time series containing a high dimensional constituent is not unique in the sense that there is a continuum of ways of extracting the coherent portion from the observed time series. A particular choice of the embedding parameters sets the complexity of the resultant dynamical model, viz. the dimension of the embedding space, and the permissible noise level. The higher the complexity is, the smaller the noise level in the system, but the larger the amount of data and thus the greater the computing power needed for constructing the dynamical model of the system. In addition to the embedding space parameters, the new technique presented in this paper also yields an estimation of the probability density function in the reconstructed phase space. Its moments yield the average dynamical properties of the system, while its evolution with input parameters gives a full description of the collective behavior in the system. Thus, it can be used to model and forecast the high dimensional portion of the observed dynamics not predicted by low dimensional deterministic models.

The next section discusses the methods of determining the minimum embedding dimensions and the necessity of introducing a new method in the case of the time series with a high dimensional component or noise. Then, we describe the method and its applications to different dynamical systems.

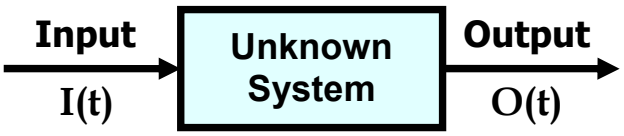

Fig. 1. Structure of an input-output system.

In Sect. 3 the embedding analyses of the $AL - vB_S$ time series are presented and the application of the probability density function to the study of the global constituent in the solar wind-magnetosphere coupling is discussed. The last section presents the main results of the paper and their implications to magnetospheric modeling.

2 Estimating the embedding dimension

A large portion of the magnetospheric dynamics is driven by the solar wind input. Therefore, the method of estimating the minimum embedding dimensions of the $vB_S - AL$ time series should be valid for non-autonomous systems. Moreover, the examination of the multi-scale properties of the solar wind-magnetosphere coupling showed (Ukhorskiy et al., 2002a) that the multi-scale constituent of the AL time series has dynamical and statistical properties similar to those of the colored noise. One of the possible origins of this multi-scale portion of AL is the scale-invariant constituent of its driver, vB_S (Freeman et al., 2000; Hnat et al., 2002). Thus, it is required that the method is also valid for the random systems, where dynamics is driven by a random process (Arnold, 1998).

There has been much work on determining the embedding dimensions of the time series generated by autonomous dynamical systems in the absence of dynamical noise (see review: Abarbanel et al., 1993). The methods developed for estimating the minimum embedding dimension are grounded on Takens' embedding theorem (Takens, 1981; Sauer et al., 1991), and most of them use the ideas of the false nearest neighbors technique (Kennel et al., 1992; Cao, 1997). Later, a number of works discussed the theoretical foundations of the delay embedding of the input-output time series (Casdagli, 1993; Stark et al., 1996). This led to the generalizations of the existing method for the case of non-autonomous dynamical systems (Rhodes and Morari, 1997; Cao et al., 1998). Recently, considerable attention was drawn to the embedding analyses of the time series generated by random dynamical systems (Muldoon et al., 1998; Stark, 2001). However, these methods are not applicable to the magnetospheric time series analysis, since they generally cannot distinguish between the pure noise and a low dimensional time series with noise contamination. Thus, for estimating the embedding dimension of the $vB_S - AL$ time series a new approach is required. In the following we discuss a new method for estimating the delay embedding parameters of random dynamical systems. The method is applicable to both autonomous and open systems, and therefore, for the sake of generality, the description will be given for the case of the input-output time series. In the case of a noise-free dynamical system, whose evolution is given by a finite set of coupled ordinary differential equations, the observed time series data is a function only of the state of the underlying system and contains all the information necessary to determine its evolution. Thus, if a space large enough to unfold the dynamical attractor is reconstructed from the time series and the present state of the system is identified, then the dynamics of the system can be inferred from the known evolution of similar states. The phase space can be reconstructed by a delay embedding method which provides the unique correspondence between the original dynamics and the dynamics in the embedding space. The embedding theorem (Takens, 1981) states that in the absence of noise, if $M \geq 2N+1$, then M-dimensional delay vectors generically form an embedding of the underlying phase space of the N-dimensional dynamical system. In the case of non-autonomous systems (Fig. 1) the M-dimensional embedding space is formed by the input-output delay vectors:

$$(\boldsymbol{I}_t^T, \boldsymbol{O}_t^T) =$$

$$(I_t, I_{t-1}, ..., I_{t-(M_I-1)}, O_t, O_{t-1}, ..., O_{t-(M_O-1)}), \quad (1)$$

where $I_t = I(t)$, $O_t = O(t)$, $M = M_I + M_O$. If the delay matrix $\mathbf{A}$ is defined as:

$$\mathbf{A} = \begin{pmatrix} \boldsymbol{I}_0^T, \boldsymbol{O}_0^T \\ . \\ . \\ . \\ \boldsymbol{I}_{Nt}^T, \boldsymbol{O}_{Nt}^T \end{pmatrix} \quad (2)$$

$$\mathbf{C} = \mathbf{A}^T\mathbf{A}; \mathbf{C}\mathbf{v}_k = w_k^2\mathbf{v}_k \in \mathbf{R}^M, k = 1, ..., M, \quad (3)$$

then $\mathbf{C}$ is the covariance matrix. Since $\mathbf{C}$ is Hermitian by definition, its eigenvectors $\{\mathbf{v}_k\}$ form an orthonormal basis in the embedding space. Vectors $\{\mathbf{v}_k\}$, which are referred to as principal components, are usually calculated by using the singular value decomposition (SVD) method, according to which any $M \times N_t$ matrix $\mathbf{A}$ can be decomposed as:

$$\mathbf{A} = \mathbf{U} \cdot \mathbf{W} \cdot \mathbf{V}^T = \sum_{k=1}^{r} w_k \cdot \mathbf{u}_k \otimes \mathbf{v}_k, \quad (4)$$

where

$$\mathbf{V} = (\mathbf{v}_1, ..., \mathbf{v}_M), \mathbf{U} = (\mathbf{u}_1, ..., \mathbf{u}_M),$$

$$\mathbf{W} = \mathrm{diag}(w_1, ..., w_M), w_1 \leq w_2 \leq ... \leq w_M$$

$$\mathbf{U} \cdot \mathbf{U}^T = 1, \mathbf{V} \cdot \mathbf{V}^T = 1.$$

The set of all delay vectors forms an irregular cloud in $\mathbf{R}^M$. If the number of delays M is greater than the minimum dimension required for the delay embedding of the observed time series, then there are directions in $\mathbf{R}^M$ into which this cloud does not extend. In this case the singular spectrum

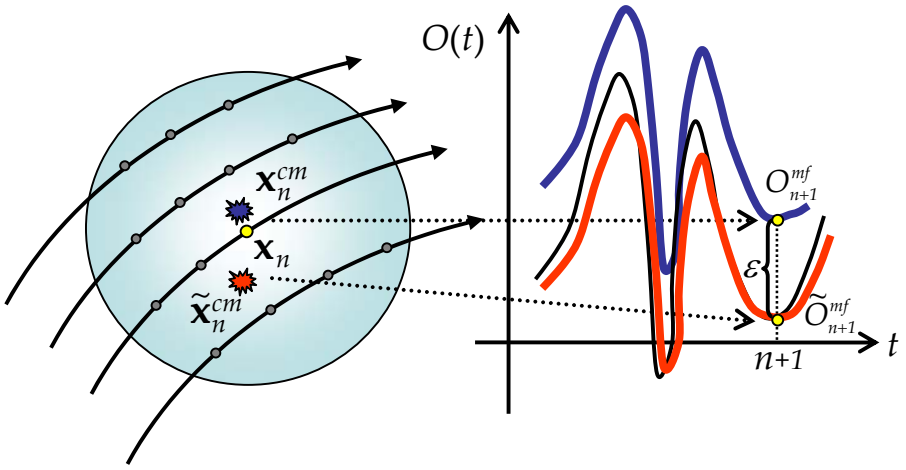

Fig. 2. Graphical representation of determining the embedding parameters of the observed time series.

analysis helps to find the subspace relevant for constructing the dynamical model of the system (Broomhead and King, 1986). The eigenvalues w_k^2 are the squared lengths of the semi-axes of the hyper-ellipsoid which best fit the cloud of data points and the corresponding eigenvectors, $\boldsymbol{v}_k$, give the directions of the axes. The most relevant directions in space are thus given by the principal components corresponding to the largest eigenvalues. Therefore, instead of the input-output delay vector (1) in the embedding space, its projection on the first D principal components:

$$\mathbf{x}_t = (\mathbf{I}_t^T, \mathbf{O}_t^T) \cdot (\mathbf{v}_1, ..., \mathbf{v}_D), \tag{5}$$

where D is the minimum embedding dimension, yields a better representation of the system. In this case, if M is substantially greater than D, small variations of M_I and M_O do not change the state of the system. For simplicity, all calculations in this paper are performed with $M_I = M_O$.

If the embedding procedure is properly performed, that is, if the attractor of the system was completely unfolded, then reconstructed states, $\mathbf{x}_n$, have a one-to-one correspondence with the states in the original phase space and thus can be used for construction of the dynamical model of the system (Farmer and Sidorowich, 1987; Casdagli, 1989, 1993; Sauer, 1993). For this purpose it is assumed that the underlying dynamics can be described as a nonlinear scalar map (6), which relates the current state to the manifestation of the following state regarding the output time series value at the next time step. The unknown nonlinear function $\mathcal{F}$ is approximated locally for each step of the map by the linear filter:

$$O_{t+1} = \mathcal{F}(\mathbf{x}_t) \approx \mathcal{F}(\tilde{\mathbf{x}}_t) + \alpha_t \cdot \delta\mathbf{x}_t, \tag{6}$$

where $\tilde{\mathbf{x}}_t$ is the expansion point. Filter coefficients are calculated using the known data, referred to as the training set, which is searched for the states similar to the current, that is, the states that are closest to it, as measured by the distance in the embedding space defined using the Euclidean metric. These states are referred to as nearest neighbors. Strictly speaking, the choice of the expansion point is somewhat arbitrary and may be different for different applications. For chaotic time series forecasting in autonomous dynamical systems Sauer (1993) suggested that better predictability is achieved when the average state vector of NN nearest neighbors $\mathbf{x}_k$, which is also called the center of mass, is taken as the center of expansion:

$$\mathbf{x}_t^{cm} = \frac{1}{NN} \sum_{k=1}^{NN} \mathbf{x}_k, \mathbf{x}_k \in NN. \tag{7}$$

It may appear that choosing a particular center of the expansion is an auxiliary procedure that leads only to some increase in the accuracy of the model. However, it was shown (Ukhorskiy et al., 2002a) that, in the case of the Earth's magnetosphere, and presumably for a large class of non-autonomous real systems, the expansion about the center of mass may be essential for modeling the system's dynamics with the use of local-linear filters. It allows for a separation of the regular dynamical constituent, stabilizes the prediction algorithm, and provides the basis for modeling the multi-scale dynamical features. It was also shown that, for the purpose of the long-term prediction, the right-hand side of the model (6) can be reduced to its zeroth term, i.e. the arithmetic average of the outputs corresponding to a one step iterated nearest neighbors equation:

$$O_{t+1}^{mf} = \mathcal{F}(\mathbf{x}_t^{cm}) = \langle O_{k+1} \rangle, \mathbf{x}_k \in NN. \tag{8}$$

As will be shown later, using the center of mass also plays a central role in estimating the minimum embedding dimensions of the time series generated by random dynamical systems.

In the case of a low dimensional coupled dynamical system the minimum embedding dimension of its time series can be easily inferred directly from data by determining the space where all false crossings of the orbits, which arose by virtue of having projected the attractor into a low dimensional space, that was too low, disappear. In the original false

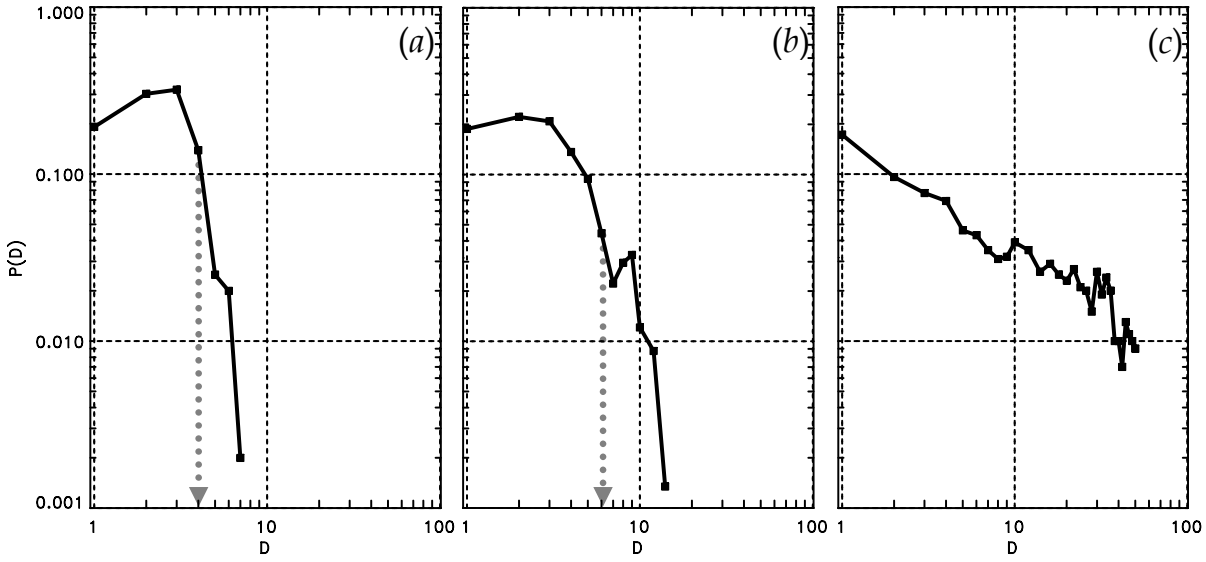

Fig. 3. Distribution functions of D_n calculated with $NN = 3$ for the time series generated by different autonomous dynamical systems. In all three cases $M_I = M + O = 50$. Grey arrows show possible choices of the embedding space dimension. **(a)** Lorenz attractor ($dt = 0.01$). Distribution function rapidly drops to zero at $D = 3 - 4$. **(b)** Mackey–Glass delay-differential equation ($dt = 0.1$). Distribution function drops to zero at $D = 6 - 7$. **(c)** $1/f$-noise generator. The power shape of the distribution function indicates the absence of finite embedding dimensions.

nearest neighbors method (Kennel et al., 1992), as well as in its generalized versions (Cao, 1997; Rhodes and Morari, 1997; Cao et al., 1998), this is done by examining whether a given state of the system and the state which was identified as its closest neighbor are nearest neighbors by virtue of the projection into a low dimensional space that was too low. The minimum dimension is assessed by examining all points of the attractor in dimension one, then dimension two, etc., until there are no incorrect or false neighbors remaining. This approach works well for determining the minimum embedding dimension of the time series generated by a wide class of autonomous and open systems in which dynamics is not subjected to noise. However, this method is not applicable to the time series generated by dynamical systems which exhibit randomness.

Let us consider the dynamics of a low dimensional system in the embedding space (assuming that the embedding procedure was performed correctly). In the absence of noise all attractor's trajectories lie on a smooth manifold. The dynamics of the system is coherent and have the same properties on all scales, starting at the largest scale given by the size of the attractor and ending at the smallest scale given by the number of data points in the training set. No two trajectories can intersect in this case, and any two states of the system can be resolved. Such system has a fixed dimension at all scales, defined by the dimension of the space which provides the embedding of the manifold containing the dynamical attractor. This picture considerably changes when noise is introduced in the system. The effect of noise is somewhat similar to a diffusion. It destroys the coherence of the dynamics on small scales, smearing the attractor points around the manifold containing "clean" dynamics. Moreover, the delay embedding in its original sense does not exist in this case, since there is no smooth manifold containing the dynamical trajectories in any finite dimension. States of the system lying within the range of scales affected by noise cannot be resolved. Thus, in this case any method similar to the false nearest neighbors, which examines the structure of the attractor on the smallest possible scale, will indicate that the system is high dimensional and a proper embedding has not been achieved. However, if the small-scale dynamical constituent affected by noise is smoothed away, then the averaged system allows for delay embedding. In random systems the range of scales in the embedding space, affected by noise depends on the noise amplitude, the inherent properties of the system and the embedding space dimension. Thus, embedding of the time series generated by random systems should be considered as a procedure of choosing the embedding space as well as determining the range of scales in this space which has to be smoothed away. In other words, introducing a probability density function on the attractor corresponding to the particular dimension of the embedding space and performing the ensemble averaging yields the smooth manifold which contains the coherent portion of the observed time series.

For a time series not contaminated by noise the criterion for a good embedding can be stated as follows. If two states $\mathbf{x}_k$ and $\mathbf{x}_n$, are close in the embedding space, then according to Eq. (6) the values of a one step iterated scalar time series corresponding to these states, O_{k+1} and O_{n+1}, should also be close. In the case of random dynamical systems this is not necessarily true, since on small scales the coherence in system's dynamics might be destroyed by noise. In this

case it is essential to not only find the dimension, but also to determine the range of scales in this space which is populated by high dimensional dynamics and thus needs to be smoothed away. For that we suggest to substitute the above criterion by the following approach. Let us consider two states $\mathbf{x}_n$ and $\mathbf{x}_k$, of the random system in the space formed by the first D eigenvectors of the covariance matrix $\{\mathbf{v}_k | k = 1, ..., D\}$, together with the sets of their nearest neighbors identified with the use of a Euclidean metric in this space. By analogy with the noise-free dynamical systems we consider this space to be an embedding space of the underlying dynamics, if there is an NN such that the following criterion is satisfied for any two states of the system:

$$\text{if} \quad \| \mathbf{x}_n^{cm} - \mathbf{x}_k^{cm} \| \to 0 \quad \text{then} \quad |O_{n+1}^{mf} - O_{k+1}^{mf}| \to 0, \quad (9)$$

where the center of mass vectors are given by Eq. (7). This condition provides that the function $\mathcal{F}$ in Eq. (8) is well defined, i.e. $\mathbf{x}_k^{cm} = \mathbf{x}_n^{cm}$ whenever $O_{k+1}^{mf} = O_{n+1}^{mf}$.

According to this definition the embedding procedure consists of finding two parameters, D and NN. If such parameters are defined, then a dynamical model of the system can be introduced in the form of Eq. (9). Averaging over NN nearest neighbors defines the smooth manifold of dimensionality D or smaller that can be fit locally to the data and then used to interpolate the dynamics of the system. As will be shown later for many random systems the choice of D and NN is not unique. In such cases D is usually a decreasing function of NN, the higher the D, the smaller the NN required for the embedding. The particular choice of the embedding parameters should be justified in each particular case by the accuracy of the dynamical model. The higher the NN, the stronger the averaging introduced into the system and thus, a larger portion of the time series is considered to be noise from the dynamical model point of view. However, it turns out that a decrease in NN does not always lead to an increase in the model's accuracy, and thus, for modeling purposes it is not always preferable to minimize it. Moreover, a decrease of NN in many cases leads to a growth of D which is necessary for a good embedding, which increases the amount of data needed and computational power required for constructing the model.

For calculation purposes the criterion (9) can also be formulated in the following way (see Fig. 2). A D-dimensional space is considered to be an embedding space, if there is a number NN such that for all points n from the data set the inclusion of the state $\mathbf{x}_n$ in the set of its nearest neighbors does not considerably change the value of the average of the outputs corresponding to a one step iterated nearest neighbors equation. In other words:

$$\| \mathbf{x}_n^{cm} - \tilde{\mathbf{x}}_n^{cm} \| \to 0 \Longrightarrow |O_{n+1}^{mf} - \tilde{O}_{n+1}^{mf}| \to 0$$

$$\mathbf{x}_n^{cm} = \frac{1}{NN} \sum_{k=1}^{NN} \mathbf{x}_k, \tilde{\mathbf{x}}_n^{cm} = \frac{1}{NN} (\mathbf{x}_n + \sum_{k=1}^{NN-1} \mathbf{x}_k), \mathbf{x}_k \in NN. \quad (10)$$

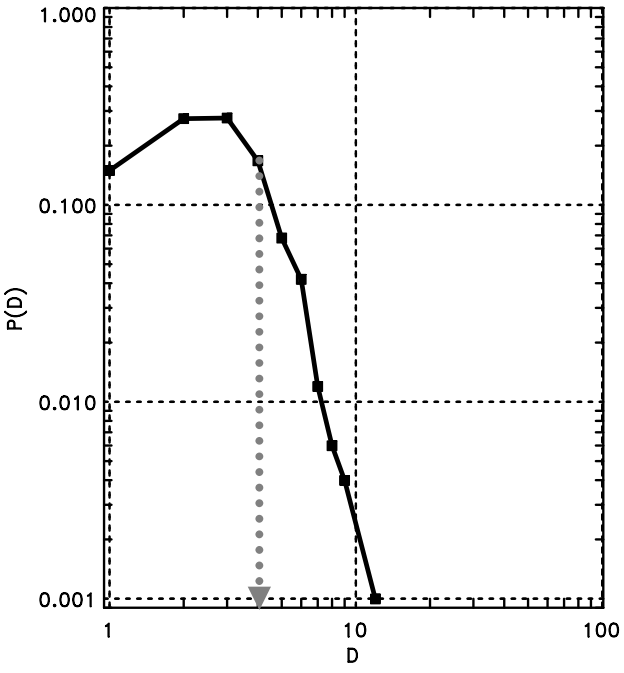

Fig. 4. Distribution functions of D_n calculated with $NN = 3$ and $M_I = M_O = 50$ for the time series generated by the synchronized Lorenz attractor. Distribution function drops rapidly to zero around $D = 4$.

Thus, for determining the optimal embedding parameters D and NN the following algorithm is proposed. First, the parameter NN is fixed at some small value. Then, for each point (I_n, O_n) of the input-output time series the conditions of criteria (10) are considered in dimension one, then dimension two, etc., until they are satisfied in some dimension D_n. In other words we seek for:

$$\min \qquad D_n : |O_{n+1}^{mf} - \tilde{O}_{n+1}^{mf}| < \varepsilon, \quad (11)$$

where ε is some small number which sets the precision in the system. Quantities differing by less than ε are considered to be identical within the permissible accuracy. When D_n is found for all points in the training set, the probability distribution of D_n is calculated. If the system has a finite embedding dimension for a chosen value of NN, then the distribution function will drop to zero at this value. If there is no finite embedding dimension for this value of NN, the distribution function has a power-law dependence. In this case NN is increased and the whole procedure is repeated until a finite dimension is found. Then, for all pairs of parameters (NN, D) the dynamical models (8) are calculated and their outputs are compared. The parameters which yield the highest accuracy of the model are considered as optimal. The delay embedding of the input-output time series generated by systems with a random component follows from dynamical systems theory based on Takens' embedding theorem. However, this technique of determining the embedding parameters is very similar to the methods known in statistical physics. This recognition can be used as a link between the

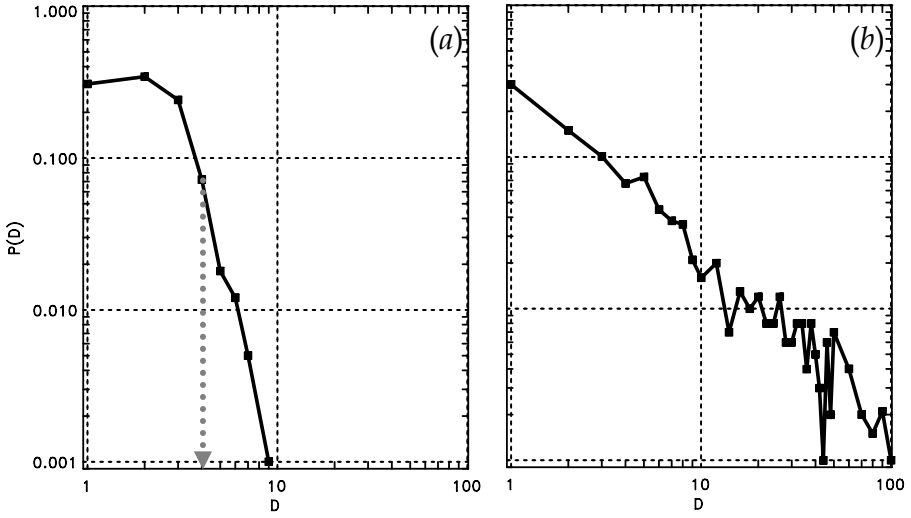

Fig. 5. Distribution functions of D_n calculated with $NN = 3$ and $M_I = M_O = 50$ for the time series generated by the synchronized Lorenz attractor with $1/f$-noise contamination. **(a)** Small noise amplitude ($\varepsilon = 0.5 > \sigma_{1/f} = 0.4$). Distribution function drops rapidly to zero at $D = 4$. **(b)** Large noise amplitude ($\varepsilon = 0.5 \ll \sigma_{1/f} = 15$). The power shape of the distribution function indicates the absence of finite embedding dimensions at the small scales.

deterministic and probabilistic approaches to modeling the collective behavior in random systems. It was pointed out earlier (Ukhorskiy et al., 2002a) that the dynamical model (8) is very similar to the mean-field approach in thermodynamics (e.g. Kadanoff, 2000), since its output is obtained by the averaging over the chosen range of scales in the reconstructed phase space. For that the reconstructed D-dimensional space is divided into the equal-probability clusters centered on every point of the data set. The size of the cluster is defined by the radius R of a sphere containing the set of NN nearest neighbors. This defines the fixed-probability partition of the phase space, which consists of a large number of overlapping clusters, all containing the same number of points but having different spatial sizes. Thus, after parameters D and NN are found the probability density function of system states in the embedding space can be estimated using the K-nearest-neighbor approach (Bishop, 1995):

$$\rho(\mathbf{x}) = \frac{\mathcal{A}}{R(\mathbf{x}, NN)^D}, \tag{12}$$

where the constant $\mathcal{A}$ is defined by the normalization condition. To obtain the model output the average is taken only over the states within a given cluster, while the states outside this cluster are considered to be independent and, therefore, do not contribute to the output. In other words, the output of the mean-field model (8) is calculated by taking the ensemble averaging with the use of the distribution function (12). From this point of view, the method presented here for determining the embedding parameters has another very transparent meaning. It assures that in the reconstructed phase space the ensemble averaging is well defined, viz. the average parameters are close to the exact parameters of the system. This also means that the mean-field approach is valid for the description of the collective behavior of the system.

Thus, the presented method can be considered as a technique of determining the mean-field dimensions of random dynamical systems, since it yields the parameters of the mean-field dynamical model, even when the embedding in its original sense does not exist, i.e. the system is high dimensional at small scales and, therefore, does not allow for the exact deterministic consideration. Before proceeding with the mean-field dimension analysis of the magnetospheric dynamics we test this method on several well-known autonomous and open dynamical systems, with and without noise. As was mention before, the calculations are not sensitive to the variations in the number of input and output delays in (1). All embedding analyses in this paper were carried out for $M_I = M_0 = 50$, and the delay time is equal to the sampling time of the time series.

2.1 Autonomous dynamical systems

In this section we determine the embedding dimensions of the time series generated by several autonomous dynamical systems like, Lorenz differential equations, Mackey–Glass delay differential equation, and $1/f$-noise generator.

2.1.1 Lorenz attractor

We consider the Lorenz equations (Lorenz, 1963):

$$\begin{cases} \dot{x}(t) = \sigma \cdot (y - x) & \sigma = 10 \\ \dot{y}(t) = r \cdot x - y - x \cdot z & r = 8/3 \\ \dot{z}(t) = -b \cdot z + x \cdot y & b = 28. \end{cases} \tag{13}$$

At the given values of parameters the system produces chaotic dynamics. The time evolution in the phase space is organized by two unstable foci and an intervening saddle point. The Lorenz attractor is a fractal set lying on the

smooth manifold embedded in three-dimensional Euclidean space. After solving the set (13) with the foorth-order Runge-Kutta, method with integral step 0.01 we apply our method of estimating mean-field dimensions to the $x(t)$ time series. Since there is no noise in the system, the reconstructed dynamical attractor should be similar to the original one and thus should have a fixed dimension on all scales. Therefore, the technique is expected to assess the minimum embedding dimension without a significant ensemble averaging. The distribution function of D_n obtained for $NN = 3$ is shown in Fig. 3a. It drops to zero rapidly at D values from 3 to 4, and, therefore, according to our method, these $D = 3 - 4$ are the good choices for the embedding dimensions of a $x(t)$ time series.

2.1.2 Mackey–Glass equation

As another example of a low dimensional dynamical system we consider the Mackey–Glass delay-differential equation (Mackey and Glass, 1977)

$$\dot{x}(t) = \frac{a \cdot x(t-\tau)}{1 + x^c(t-\tau)} - b \cdot x(t). \quad (14)$$

The Mackey-Glass equation is, in principal, infinite-dimensional, in the sense that a future value depends on a continuum of past values. It was shown, however, that for the parameter values of $a = 0.2$, $b = 0.1$, $c = 10$, and $\tau = 30$ the system becomes chaotic with a fractal dimension of about 3.6 (Meyer and Packard, 1992). The equation was solved with the fourth-order Runge-Kutta method, with integral step 0.1. The embedding analyses showed that at these parameter values the dynamical attractor can be embedded in 6-dimensional space (Mead et al., 1992). As in the case of the Lorenz attractor, no averaging is required to determine the minimum embedding dimension. For $NN = 3$ the D_n distribution function rapidly drops to zero at D, to about 6–7 (Fig. 3b), and, therefore, good choices for embedding dimension are $D = 6$ or 7.

2.1.3 $1/f$-noise

To illustrate what happens if the above analysis is applied to a high dimensional system, we consider the $1/f$-noise time series, viz. the time series produced by a random number generator, where the power spectrum drops with an increase in frequency as $1/f$. The D_n distribution function calculated for $NN = 3$ is shown in Fig. 3c. The distribution function has a power dependence on D in the wide range of dimensions ($D = 1-100$). This indicates that for the given averaging the system does not have a finite mean-field dimension. Since in this case almost no averaging was done ($NN = 3$), the power shape of the distribution function also means that the observed time series does not allow for the delay embedding in the sense of the original noise-free embedding theorem.

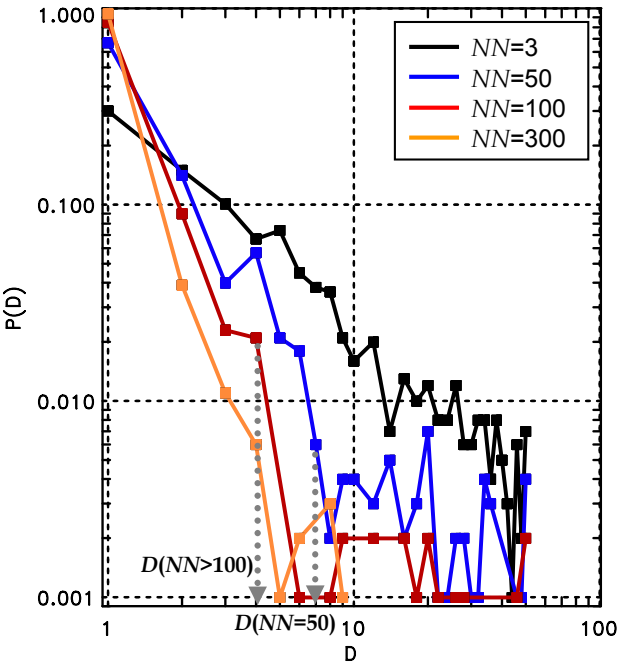

Fig. 6. Distribution functions of D_n calculated with $\varepsilon = 0.5$ and different values of NN for the time series generated by the synchronized Lorenz attractor with $1/f$-noise contamination ($\sigma_{1/f}$). For different NN the distribution function drops to zero at different values of D. The mean-field dimension decrease with the increase in the range of scale smoothed away after the averaging.

2.2 Input-output time series

Before proceeding with the analysis of noise effects on the delay embedding, we present an example of determining the embedding dimensions of the input-output time series. As an example of a non-autonomous, low dimensional dynamical system we consider a synchronized Lorenz attractor. If the $x(t)$ component of one Lorenz system is used as a driver for the second Lorenz system, then the attractors of both systems synchronize at the following values of parameters: $r = 60$, $b = 8/3$, $\sigma = 10$ (Pecora and Carroll, 1990), i.e. independent of the initial conditions of the second system; after a few steps its trajectory converges to the attractor of the driver. Thus, the $Y(t)$ component of the second Lorenz attractor can be considered as an output of the non-autonomous chaotic dynamical system driven by the input $-x(t)$ component of the first Lorenz attractor. The distribution function of D_n calculated for $NN = 3$ is shown in Fig. 4. The rapid drop in the distribution function indicates that $D = 3 - 4$ are good choices for embedding dimensions of the input-output time series.

2.3 Noise effects

The examples of the time series presented above were generated by low dimensional dynamical systems (except for the $1/f$-noise case). Consequently, the mean-field dimensions of

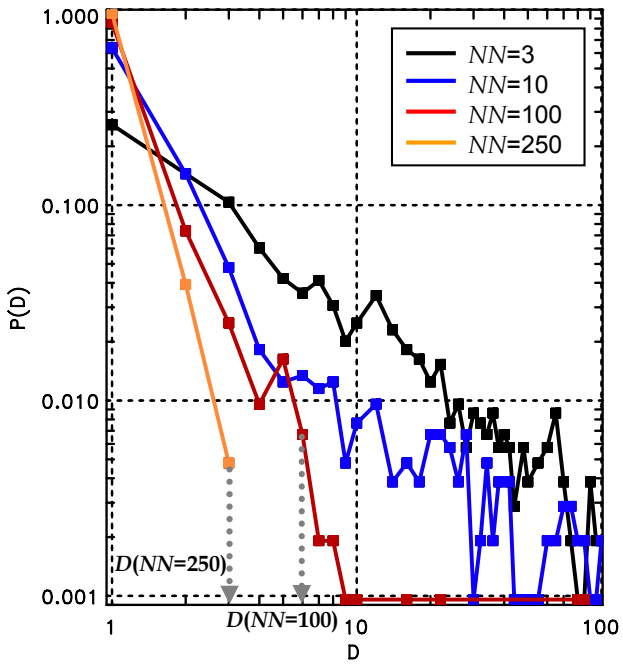

Fig. 7. Distribution functions of D_n calculated with different values of NN for $vB_S - AL$ time series of Bargatze et al. (1985) database. For different NN the distribution function drops to zero at different values of D. The mean-field dimension decrease with the increase in the range of scale smoothed away after the averaging.

these systems were determined with almost no averaging and thus do not differ from the minimum embedding dimensions found with the use of other methods, like the false nearest neighbors technique. In this section we consider the effects of noise on the embedding analysis of the observed time series. It is shown that, in the presence of a significant noise component, the delay embedding becomes possible only after averaging the data in the reconstructed phase space. To study the effects of noise on delay embedding we consider the input-output time series of the synchronized Lorenz attractor contaminated by a $1/f$-noise time series of various amplitudes. The noise amplitude is considered to be small if $\varepsilon > \sigma_{1/f}$, where $\sigma_{1/f}$ is the variance of the noise time series. The distribution function of D_n calculated for the small noise contamination with $NN = 3$ is shown in Fig. 5a. As can be seen from the plot the distribution function does not differ much from the distribution function calculated for the clean time series of the synchronized Lorenz attractor (Fig. 4). Since almost no averaging was done, the sharp drop in the distribution function indicates the existence of low dimensional embedding space ($D = 3-4$) at the smallest interaction scales. However, this low dimensional picture significantly changes when the amplitude of the noise is substantially increased ($\varepsilon \ll \sigma_{1/f}$). In this case the D_n distribution function calculated for $NN = 3$ has a power shape similar to the distribution function calculated for the $1/f$-noise time series (Fig. 5b, Fig. 3c). This means that in the embedding space of any dimension the coherent, low dimensional dynamics of the system appears to be destroyed by the noise within some range of scales. Thus, at small scales the dynamical properties of the systems are indistinguishable from those of the noise itself. This also limits the information that can be extracted by exploring the dynamical trajectories on the smallest scales.

To extract more information about the system's dynamics and, in particular, to obtain the range of scales affected by noise, we follow the prescription of our method and increase the number of nearest neighbors participating in the averaging. Figure 6 shows the D_n distribution functions calculated for different values of NN. It is seen from the plots that starting at $NN = 50$ the averaged systems start exhibiting a low dimensional behavior. The particular values of dimensions correspond to the minimum embedding dimensions of the averaged dynamical systems, where the degree of averaging is set by NN. The small-scale portion of the time series which is smoothed away due to the averaging is not embedded in this particular dimension. Therefore, the assessed dimensions should be considered only as the mean-field dimensions of the system. At $NN = 50$, $D = 7$ and for $NN > 100$, $D = 4$.

To distinguish the pair of parameters which is optimal for the embedding of the observed time series we use these parameters to build a dynamical model in the form of (8). The optimal parameters are identified as those which provide the highest prediction accuracy of the model. Throughout this paper the prediction accuracy of dynamical models is quantified by the normalized mean squared error ($NMSE$) (Gershenfeld and Weigend, 1993)

$$NMSE = \frac{1}{\sigma_O}\sqrt{\frac{1}{N}\sum_{k=1}^{N}(O_k - \hat{O}_k)^2}. \qquad (15)$$

Here, $k = 1$ to N span the forecasting interval, σ_O is the standard deviation of the original output time series, and the $\hat{}$-symbol denotes the predicted values. The value $NMSE = 1$ corresponds to a prediction of the average. For (D, NN) of (7, 50) $NMSE = 0.9$ and for (4, 100) $NMSE = 0.8$. Therefore, according to our method the optimal embedding parameters (D, NN) of the input-output time series generated by the contaminated synchronized Lorenz system are (4, 100).

After the embedding parameters (D, NN) of the time series are determined, the probability density function on the dynamical attractor can be introduced in the form of Eq. (12). Since it is a distribution function in the reconstructed D-dimensional phase space, it yields the average properties of the system and provides the basis for a probabilistic description of its dynamics. Different aspects of applying the distribution function to study the evolution of the system in the embedding space will be considered in the next sections, where the embedding analysis of magnetospheric dynamics is discussed.

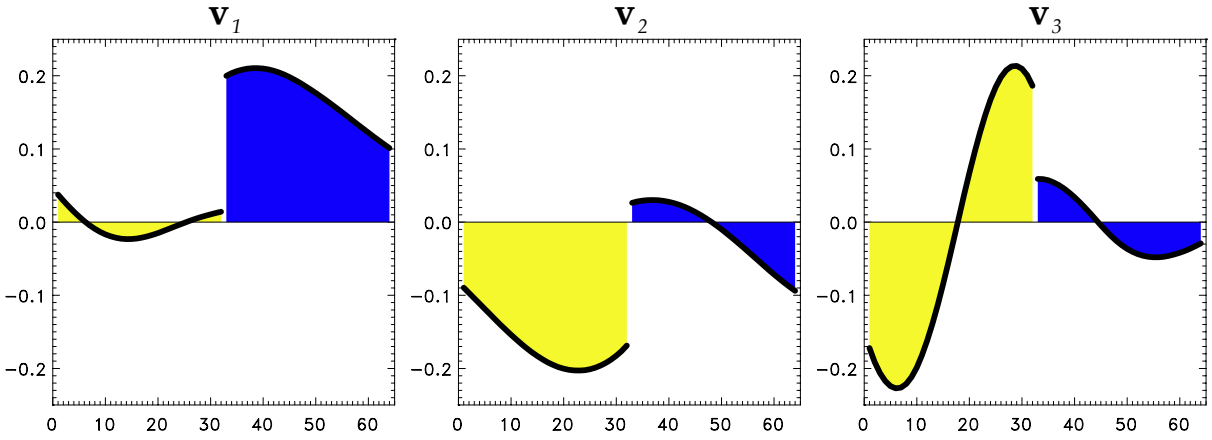

Fig. 8. The first three principal components of $vB_S - AL$ covariance matrix computed with $M_I = M_O = 32$. The input (vB_S) portion of vector is shown in yellow, while the output (AL) part is indicated by the blue color.

3 Embedding analyses of magnetospheric dynamics

Previous studies pointed out that the magnetospheric dynamics has different properties at different scales. The dimension analysis of AE data (Vassiliadis et al., 1990) showed that the correlation dimension saturates at low values, which indicates the global nature of substorm dynamics. It was also shown that a large portion of the AE time series can be described by low dimensional dynamical models (Vassiliadis et al., 1995). However, it was also demonstrated that if all interaction scales are taken into account, then the AE time series does not have a low correlation dimension (Prichard and Price, 1992). Using the coast-line dimension analysis Sitnov et al. (2000) showed that the low dimensional behavior can be derived only for the fixed range of the largest perturbation scales, while the singular value spectrum of data has a power-law shape typical for the colored noise. The subsequent analyses of the multi-scale constituent of AL also indicated that it has dynamical and statistical properties similar to the time series of high dimensional noise (Ukhorskiy et al., 2002a).

The main goal of our work is to develop a comprehensive model that can account for both global and high dimensional constituents of the solar wind-magnetosphere coupling during substorms. The basis of this model is provided by the embedding analysis discussed in previous sections. Our method yields the mean-field dimensions of the system that are used for constructing low dimensional dynamical model to run iterative predictions of the observed time series (Ukhorskiy et al., 2002a). Moreover, it also yields the distribution function of the high dimensional dynamical constituent in the reconstructed phase space. In this section we show how this distribution function can be used for studying the structure of a low dimensional dynamical attractor and discuss its application to probabilistic predictions of the magnetospheric dynamics.

Previous studies of the solar wind-magnetosphere coupling discussed different choices of the solar wind input parameters for the magnetospheric dynamics. For the modeling of AL and AU indices Clauer et al. (1981) considered the solar wind convective electric field vB_S, v^2B_S and the solar wind coupling parameter $\varepsilon = vB^2l_0^2\sin^4(\theta/2)$ (Akasofu, 1979). They found that the moving average linear filters based on these three inputs have the similar prediction accuracy of 40%. Vassiliadis et al. (1995) reported that the local-linear filters driven by vB_S, $vB^2l_0^2\sin^4(\theta/2)$ and vB_z yield a comparable predictability of AL. For the predictions of high geomagnetic activity the best results were achieved with unrectified vB_z input. In this study the solar wind input is quantified by vB_S, while the magnetospheric response is represented by the AL index. This allows for the direct comparison of our embedding analysis with earlier results of Sitnov et al. (2000, 2001), obtained for $vB_S - AL$ time series. All analyses were carried out using the correlated database of solar wind and geomagnetic time series compiled by Bargatze et al. (1985). The data are solar wind parameters acquired by IMP 8 spacecraft and simultaneous measurements of auroral indices with a resolution of 2.5 minutes. The database consists of 34 isolated intervals, which contain 42 216 points in total. Each interval represents the isolated interval of auroral activity preceded and followed by at least two-hour-long quiet periods ($vB_S \approx 0$, $AL < 50$ nT). Data intervals are arranged in the order of increasing geomagnetic activity. In order to use both vB_S and AL data in joint input-output phase space, their time series are normalized to their standard deviations.

To determine the mean-field dimensions of the magnetospheric dynamics we follow the prescription of our method and estimate the embedding dimensions of the $vB_S - AL$ time series after carrying out the ensemble averaging in the embedding space. The distribution functions of D_n are calculated for different values of NN, which set the range of scales participating in the averaging (Fig. 7). The distribution function calculated for averaging over $NN = 3$ has a power-law shape. This indicates that at the finest scales the

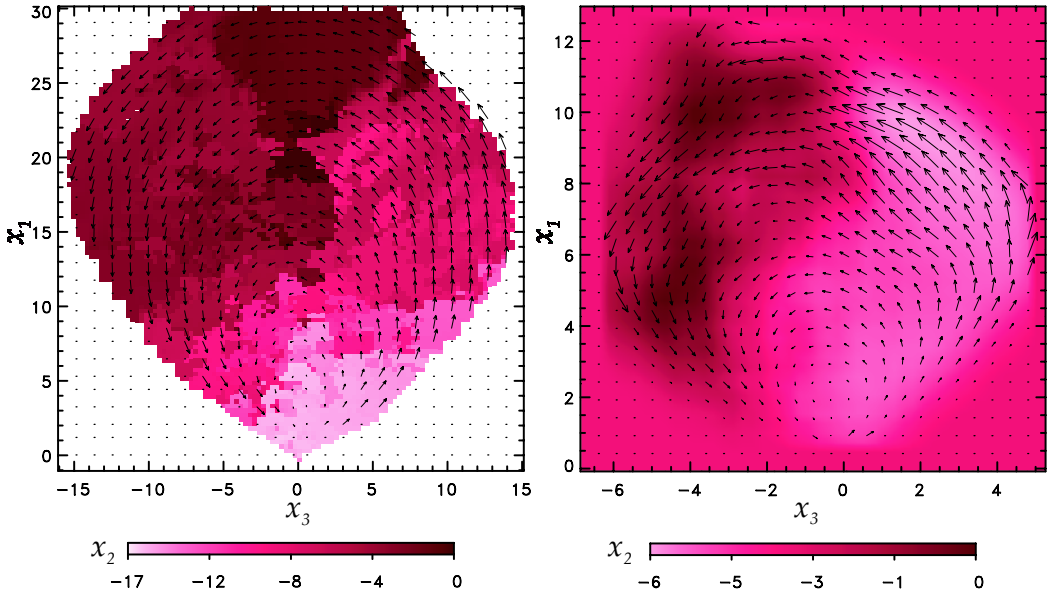

Fig. 9. The coherent dynamics in three-dimensional subspace spanned by the leading principal components of $vB_S - AL$ covariance matrix. **(a)** The dynamical manifold is derived with the use of the two-dimensional distribution function $\rho(x_1, x_3)$ calculated for the whole Bargatze et al. (1985) database with $NN = 300$. The points of the surface are associated with the maxima of the conditional probability function $\rho(x_2|x_1, x_3) \cong \rho(x_2^{(k)})$. **(b)** Smoothed dynamical manifold calculated for the first 20 intervals of Bargatze et al. (1985) database by Sitnov et al. (2001).

dynamics in the system is irregular and cannot be embedded in a finite-dimensional space. Only after a substantial range of scales is smoothed away ($NN > 100$) does the averaged system start to exhibit a low dimensional behavior. Thus, for $NN = 100$ the mean-field dimension is $D = 7$, and for $NN = 250$, $D = 3$. To define which embedding parameters are optimal for modeling the evolution of the system we construct the dynamical model (8) and then calculate $NMSE$ for different values of (D, NN). For (3, 250) $NMSE = 0.63$ and for (7, 100) the error value is smaller, $NMSE = 0.57$.

After the optimal embedding parameters (D, NN) are chosen, the probability density function of the attractor states can be estimated as Eq. (12). Since it is a distribution function in D-dimensional reconstructed phase space, it can be used for studying the collective behavior of the system. The global dynamics of the system is described by the moments of the distribution function. Thus, the zeroth order term in dynamical model (8), viz. the center of mass, is nothing but its first moment. The distribution function can also be used for visualizing the low dimensional component of the solar wind-magnetosphere coupling. Earlier procedures of visualizing the global part of the magnetospheric dynamics (Sitnov et al., 2000; Sitnov et al., 2001) involved a number of cumbersome procedures, such as the removal of the hysteresis loops and the smoothing of the resultant 2-D surface. Our new systematic approach resolves these problems by substituting the raw data by its probability density function in the reconstructed space, whose dimension is consistent with the level of averaging and the level of noise. To compare our results with the phase portrait obtained by Sitnov et al. (2001), we plot the data in three-dimensional space given by the principal components $\mathbf{v}_1$, $\mathbf{v}_2$ and $\mathbf{v}_3$ of $vB_S - AL$ covariance matrix. For a better comparison the principal components were calculated for the matrices computed with the same $M_I = M_O = 32$ number of delays as was used by Sitnov et al. (2001). Vectors $\mathbf{v}_1$, $\mathbf{v}_2$ and $\mathbf{v}_3$ are shown in Fig. 8. The delay vector projections x_1 , x_2 and x_3 onto $\mathbf{v}_1$, $\mathbf{v}_2$ and $\mathbf{v}_3$ roughly correspond to one-hour average values of input (normalized vB_S), output (normalized AL) and the first time derivative of the input (for details, see Sitnov et al., 2000). To visualize the data we use $x_1 - x_3$ projection as the support plane, where the distribution function $\rho(x_1, x_3)$ is introduced according to Eq. (12), with $NN = 300$ obtained by the mean-field dimension analysis. Then, at any given point (x_1, x_3) the conditional probability function of x_2 can be estimated as the probability density function of $x_2^{(k)}$ corresponding to the nearest neighbors of that point:

$$\rho(x_2|x_1, x_3) \cong \rho(x_2^{(k)}), \qquad \mathbf{x}_k = (x_1^{(k)}, x_3^{(k)}) \in NN. \quad (16)$$

The points of conditional probability maxima calculated at the mesh points of the regular grid set represent the surface corresponding to the most probable states of the system in three dimensional phase space. Such a surface calculated for the whole Bargatze database is presented in Fig. 9a. To visualize the evolution of the system along this surface we plot a two-dimensional velocity field, viz. the average flow velocity in a $x_1 - x_2$ plane calculated using the distribution function $\rho(x_1, x_2)$. As can be seen from the plot the structure of the surface and the corresponding circulation flows are very similar to those obtained by Sitnov et al. (2000). This similarity

is even more notable, since the phase portrait on the right was derived only for the first 20 intervals of the database, corresponding to the low and medium levels of substorm activity. At the same time, the robustness of our technique yields the phase portrait for the whole data containing both low and high activity intervals. The most probable substorm cycles are confined to the two-level surface, with the fracture going roughly along the $x_3 = 0$ axis. Two levels of the surface can be associated with the ground and exited states of the system. The typical substorm cycle starts with an increase in the average input x_1, while the average output x_2 is constant or slowly decreasing, viz. the system is in its ground state. At the same time the average input rate x_3 first increases and then decreases to small values. Then the output component falls rapidly to negative values at almost constant input parameters, which corresponds to the transition to the exited state. The recovery of the system to its ground state involves the decrease in x_1 while the magnitude of x_3 first increases and then falls to zero values.

It was pointed out before (Sitnov et al., 2000) that both the surface and the corresponding circulation flows are close to the scheme of the inverse bifurcation (Lewis, 1991). This implies that the smooth manifold underlying the global portion of system's dynamics has a folded structure known in mathematics as a cusp catastrophe manifold (Gilmore, 1993) and in the physics of non-equilibrium phase transitions as a coexistence surface separating deferent states of matter (Gunton et al., 1983). In the case of the quasi-static phase transitions in equilibrium systems the corresponding coexistence surface does not have such a folded structure. In these systems the order parameter is a single-valued function of control parameters (Fig. 10). The fold appears only in the non-equilibrium case, when the system is driven far from the steady-state equilibrium by the rapid changes in the control parameters. As a result the metastable states, like "overcooled" steam and "overheated" fluid, become possible and depending on its dynamical history, the system may be in two or more different states under the same set of control parameters. This dynamical phenomenon known as hysteresis explains the observed irregular structure of the transition line (see Fig. 9a). It also strongly complicates the reconstruction and visualization of the global dynamical constituent (Sitnov et al., 2000). In the present approach this problem is overcome with the use of the distribution function. To visualize the large-scale behavior we follow the dynamics of the distribution function maxima which is somewhat analogous to the Maxwell convention in bifurcation theory (Gilmore, 1993) and thus establishes the parallel with the equilibrium coexistence surface. The existence of the multiple maxima is attributed to the dynamical hysteresis. The points on the surface corresponding to the transitions between the ground and exited states are identified by the change in the position of the global maxima. Figure 11 shows the distribution function of x_2 calculated at three points along the cut of the surface by the $x_1 = 9$ plane. In all three cases it has a typical double-peak structure which indicates the existence of hysteresis. Figure 10 illustrates the system's transition from the ground

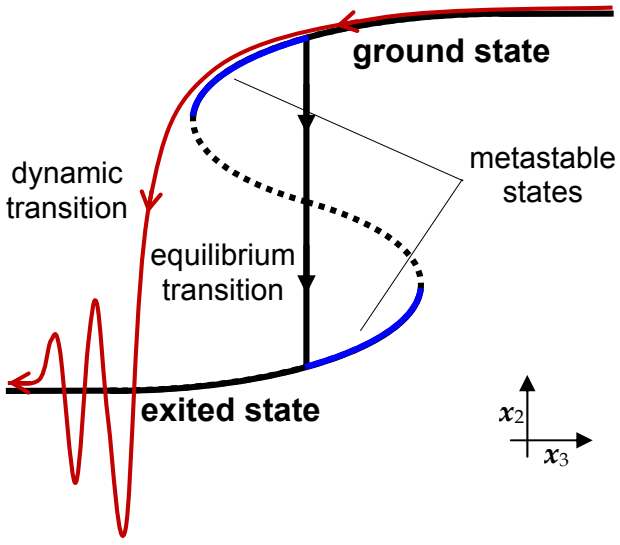

Fig. 10. The diagram of different transitions in a two-level system. The coexistence manifold and corresponding transitions from the ground to the exited state are shown in $x_1 - x_3$ plane. Equilibrium transitions correspond to the straight line connecting two branches associated with different states. The metastable states correspond to the blue segments of the manifold. An example of a typical dynamic transition which deviates from the equilibrium manifold is shown in red.

to the exited state, as identified by changes in the shape of the distribution function. According to criterion (15) the distribution function in Fig. 10c corresponds to the ground state of the system. The distribution function in Fig. 10b corresponds to the moment when the transition to the exited state was just made. And finally, the function in Fig. 10a corresponds to the fully developed exited state of the system. Thus, the distribution function and its moments can be effectively used to predict, visualize and analyze the global portion of the solar wind-magnetosphere coupling. Moreover, the description provided by the distribution function is not restricted to the low dimensional dynamical constituent. Indeed, if the distribution function and its evolution with the input parameters are derived from the observed time series, then, in principal, it gives the full description of the collective behavior in the system. The dynamics of its first moment corresponds to the mean-field dynamical model, which yields iterative predictions of the observed time series. As was discussed before (Ukhorskiy et al., 2002a), the dynamical model leaves out a significant portion of the dynamics. Indeed, in order to extract the coherent component from the time series generated by a system with some randomness, the model is forced to carry out the phase space averaging over a wide range of scales. Therefore, the output of the model comes inherently smoothed and cannot grasp the large peaks and sharpest changes in data. As will be discussed in forthcoming publications this problem can be partially resolved with the use of a distribution function, which yields the probabilistic description of the multi-scale dynamical constituent. It can be

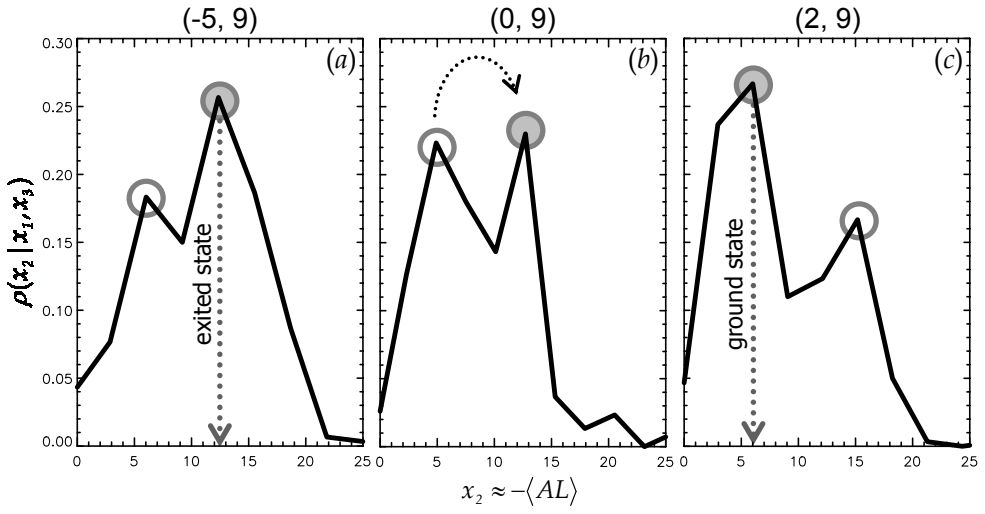

Fig. 11. Evolution of the distribution function at the different stages of substorm. Double-peak shape of the function indicate the existence of dynamical hysteresis. **(c)** The dominance of the left maximum indicates that the system is in the ground state (growth phase). **(b)** The equality of the maxima corresponds to the transition from the ground to the exited state (expansion phase). **(a)** Predominance of the right maximum indicates that the system is in the exited stated (late expansion or early recovery phases).

used to estimate the deviation of the data from the output of the deterministic model and thus can be used for probabilistic predictions. Incorporating this distribution function in the space weather prediction tools has important implications for space weather forecasting.

4 Conclusions

The solar wind-magnetosphere coupling during substorms exhibits dynamical features in a wide range of spatial and temporal scales. The large-scale portion of the magnetospheric dynamics is coherent and well organized, while many small-scale phenomena appear to be multi-scale. Most of the contemporary approaches to the data-derived modeling of magnetospheric substorms do not account for the coexistence of global and multi-scale phenomena and thus do not provide a complete description of the observed time series. Low dimensional dynamical models effectively extract the time series constituent generated by the large-scale coherent behavior, but are unable to predict the features associated with high dimensional multi-scale dynamics. At the same time, SOC-like models can reproduce a variety of the scale-free power spectra typical for the multi-scale portion of the observed time series, but are incapable of relating them to the specific global features of the actual magnetospheric dynamics and variations in the solar wind input. The goal of our work is to combine the global and multi-scale features of the solar wind-magnetosphere coupling in a single data-derived model. For this purpose we combined the deterministic methods of nonlinear dynamics with the distribution function technique of statistical physics. In this paper we analyzed to what extent the magnetospheric dynamics can be predicted with the use of the low dimensional dynamical models and at what point the statistical description is required. This question was addressed by embedding analyses of $vB_S - AL$ time series. A large portion of magnetospheric dynamics is driven by the solar wind input whose time series have scale-free power spectra. Thus, for its embedding analyses we introduce a new method of determining the embedding parameters of the input-output time series generated by random dynamical systems. To test our method we used several well-known autonomous as well as input-output dynamical systems, with and without noise contamination.

According to our embedding analysis, the multi-scale properties of the $vB_S - AL$ time series are very different from the multi-scale properties of low dimensional chaotic systems, like the Lorenz attractor or Mackey-Glass system, in which the scale-invariance is reconciled with low dimensionality due to the fractal nature of their attractors. Due to the scale-invariance of its driver and/or due to its own complexity, the magnetospheric dynamics generate time series which contain a small-scale component with properties of high dimensional colored noise. This high dimensional constituent destroys the coherence of the system's dynamics in the phase space, smearing trajectories in some vicinity of the manifold containing the dynamical attractor. Thus, if the time series are considered at the smallest possible scale, they do not allow embedding in any finite dimension. To extract the large-scale regular component from the time series, the ensemble averaging over a number (NN) of nearest neighbors, which defines the range of scales affected by noise in D-dimensional embedding space, is carried out. This smoothes away the small- scale high dimensional component and unfolds the trajectories of the averaged system in D-dimensional embedding space. The higher the value of NN, the wider the range of scales which are smoothed away and the smaller the effective dimension D of the aver-

aged system. Thus, a single set of parameters (D, NN) corresponding to the reconstruction of the "correct" dynamical system does not exist. The delay embedding should be seen rather as a process of striking a balance between the level of "noise" (the range of scales over which the averaging is performed) and the complexity (the effective dimensionality of the averaged system). Similar conclusions were reached by Stark (2001) from the theoretical analysis of the delay embedding of stochastic dynamical systems. The particular choice of the embedding parameters should be justified in each particular case by the accuracy the of dynamical model. Since these embedding parameters correspond to the averaged system rather than to the original time series and since they are directly used in the mean-field model of the system, it is more appropriate to consider D as the mean-field dimension of the system.

After the optimal embedding parameters (D, NN) are chosen, a distribution function is introduced in D-dimensional phase space. It evolves in time due to the variation of the input parameters. The dynamics of its first moment corresponds to the mean-field model of the system, which describes the low dimensional portion of the observed time series. The distribution function can also be used for visualization of the low dimensional dynamical constituent, even in the presence of noise and other non-equilibrium features, such as the hysteresis phenomenon. As was revealed by the distribution function maxima, the global constituent of the solar-wind magnetosphere coupling resembles the dynamics of non-equilibrium phase transitions. When viewed in three-dimensional subspace, given by the leading eigenvectors of the covariance matrix, the dynamics is organized around the manifold similar to the "pressure-temperature-density" coexistence surface of liquid-gas systems or to the solution of the equilibrium Ising model of ferromagnets. The substorm onset corresponds to the jump in the system between the points of the metastable and stable equilibrium, similar to the first order phase transition. The typical two-peak shape of the distribution function observed at the region of transition indicates the existence of dynamical hysteresis which confirms the non-equilibrium nature of the transition.

In the reconstructed embedding space the multi-scale constituent of the magnetospheric dynamics is naturally coupled to the large-scale regular component. It appears as fluctuations of data around the smooth manifold containing the trajectories of an averaged system, which are also described by the distribution function. Thus, the distribution function provides the full description of the collective behavior in the system. Its first moment describes the global portion of the solar wind-magnetospheric coupling and thus can be used to forecast the low dimensional trend of the observed time series. Moreover, as will be shown in following publications, if the distribution function dependence from input parameters is derived from data, then it can be used for predictions of the multi-scale dynamical constituent. Therefore, further improvements in space weather forecasting tools may be achieved by a combination of the dynamical description for the global component and a statistical approach for the multi-scale component.

Acknowledgements. The research is supported by NSF grants ATM-0001676 and ATM- 0119196, and NASA grant NAG-5111.

Topical Editor T. Pulkkinen thanks two referees for their help in evaluating this paper.

References

Abarbanel, H. D., Brown, R., Sidorovich, J. J., and Tsimring, T. S.: The analysis of observed chaotic data in physical systems, Rev. Mod. Phys., 65, 1331, 1993.

Akasofu, S.-I.: Interplanetary energy flux associated with magnetospheric substorms, Planet. Space Sci., 27, 425, 1979.

Angelopoulos, V., Mukai, T., and Kokubun, S.: Evidence for intermittency in Earth's plasma sheet and implications for self-organized criticality, Phys. Plasm., 6, 4161, 1999.

Arnold, L.: Random dynamical systems, Springer-Verlag, New-York, 1998.

Bak, P., Tang, C., and Wiesenfeld, K.: Self-organized criticality: An explanation of $1/f$ noise, Phys. Rev. Lett., 59, 381, 1987.

Bargatze, L. F., Baker, D. N., McPherron, R. L., and Hones, E. W.: Magnetospheric impulse response for many levels of geomagnetic activity, J. Geophys. Res., 90, 6387, 1985.

Bishop, C. M.: Neural Networks for Pattern Recognition, Oxford University Press Inc., New York, 1995.

Borovsky, J. E., Elphic, R. C., Funsten, H. O., and Thomsen, M. F.: The Earth's plasma sheet as a laboratory for flow turbulence in high-β MHD, J. Plasma Phys., 57, 1, 1997.

Broomhead, D. S. and King, G. P.: Extracting qualitative dynamics from experimental data, Physica D, 20, 217, 1986.

Cao, L., Mees, A., Judd, K., and Froyland, G.: Determining the minimum embedding dimensions of input-output time series, IJBC, 8, 1491, 1998.

Cao, L.: Practical method for determining the minimum embedding dimension for a scalar time series, Physica D, 110, 43, 1997.

Casdagli, M.: A dynamical approach to modeling input-output systems, in: Time Series Prediction: Forecasting the Future and Understanding the Past, Santa Fe Institute Studies in the Science of Complexity XV, edited by Weigend, A. S. and Gershenfeld, N. A., Addison-Wesley, Reading, MA, 1993.

Casdagli, M.: Nonlinear prediction of chaotic time series, Physica D, 35, 335, 1989.

Chakrabarti, B. K. and Acharyya, M.: Dynamic transitions and hysteresis, Rev. Mod. Phys., 71, 847, 1999.

Chang, T.: Self-organized criticality, multi-fractal spectra, sporadic localized reconnections and intermittent turbulence in the magnetotail, Phys. Plasmas, 6, 4137, 1999.

Chapman, S. C.: Inverse cascade avalanche model with limit cycle exhibit limiting period doubling, intermittency, and self similarity, Phys. Rev. E, 62, 1905, 2000.

Chapman, S. C., Watkins, N. W., and Rowlands, G.: Signature of dual scaling in a simple avalanche model of magnetospheric activity, JASTP, 63, 1361, 2001.

Chapman, S. and Watkins, N.: Avalanching and self-organized criticality, a paradigm for geomagnetic activity? Space Science Reviews, 95, 293, 2001.

Clauer, C. R., McPherron, R. L., and Searls, C.: Solar wind control of auroral zone geomagnetic activity, Gephys. Res Lett., 8, 915, 1981.

Consolini, G. and Lui, A. T. Y.: Sign-singular analysis of current disruption, Geophys. Res. Lett., 26, 1673, 1999.

Consolini, G., Marcucci, M. F., and Candidi, M.: Multifractal structure of auroral electrojet index data, Phys. Rev. Lett., 76, 4082, 1996.

Consolini, G. and Michelis, P. D.: A revised forest-fire cellular automaton for the nonlinear dynamics of the Earth's magnetotail, JASTP, 63, 1371, 2001.

Consolini, G.: Sandpile cellular automata and magnetospheric dynamics, in: Cosmic Physics in the Year 2000, Proc. Vol. 58, edited by Aiello, S., Iucci, N., Sironi, G., Traves, A., and Villante, U., SIF, Bologna, Italy, 1997.

Drossel, B. and Schwabl, F.: Self-organized criticality in a forest-fire model, Physica A, 191, 47, 1992.

Farmer, J. D. and Sidorowich, J. J.: Predicting chaotic time series, Phys. Rev. Lett., 59, 845, 1987.

Freeman, M. P., Watkins, N. W., and Riley, D. J.: Evidence for a solar wind origin of the power law burst lifetime distribution of the AE index, Geophys. Res. Lett., 27, 1087, 2000.

Gershenfeld, N. A. and Weigend, A. S.: Forecasting the Future and Understanding the Past, in: Time Series Prediction, Santa Fe Institute Studies in the Science of Complexity, XV, edited by Weigend, A. S., and Gershenfeld, N. A., Addison-Wesley, Reading, MA, 1993.

Gilmore, R.: Catastrophe Theory for Scientists and Engineers, Dover, Mineolta, New York, 1993.

Gleisner, H. and Lundstedt, H.: Response of the auroral electrojets to the solar wind modeled with neural networks, J. Geophys. Res., 102, 14 269, 1997.

Grassberger, P. and Procaccia, I.: Measuring the strangeness of strange attractors, Physica D, 9, 189, 1983.

Gunton, J. D., Miguel, M. S., and Sahni, P. S.: The dynamics of first-order phase transitions: Phase Transitions, Volume 8, 267, Academic Press London, 1983.

Hernandes, J. V., Tajima, T., and Horton, W.: Neural net forecasting for geomagnetic activity, Geophys. Res. Lett., 20, 2707, 1993.

Hnat, B., Chapman, S. C., Rowlands, G., Watkins, N. W., and Freeman, M. P.: Acaling of solar wind ε and the AU, AL and AE indices as seen by WIND, Geophys. Res. Lett., 29(22), 2078, doi: 10.1029/2002/GL016054, 2002.

Hohenberg, P. C. and Halperin, B. I.: Theory of dynamic critical phenomena, Rev. Mod. Phys., 49, 435, 1977.

Horton, W., Smith, J. P., Weigel, R., Crabtree, C., Doxas, I., Goode, B., and Cary, J.: The solar-wind driven magnetosphere-ionosphere as a complex dynamical system, Phys. Plasm., 6, 4178, 1999.

Ieda, A., Mashida, S., Mukai, T., Saito, Y., Yamamoto, T., Nishida, A., Terasawa, T., and Kokubun, S.: Statistical analysis of the plasmoid evolution with Geotail observations, J. Geophys. Res., 103, 4453, 1998.

Kadanoff, L. P.: Statistics Physics: Statics, Dynamics and Renormalization, World Scientific Publishing Co. Pte. Ltd., 2000.

Kennel, M., Brown, R., and Abarbanel, H.: Determining embedding dimension for phase space reconstruction using a geometrical construction, Phys. Rev. A, 45, 3403, 1992.

Klimas, A. J., Vassiliadis, D., Roberts, D. A., and Baker, D. N.: The organized nonlinear dynamics of the magnetosphere (an invited review), J. Geophys. Res., 101, 13 089, 1996.

Klimas, A. J., Vassiliadis, D., and Baker, D. N.: Data-derived analogies of magnetosphere dynamics, J. Geophys. Res., 102, 26 993, 1997.

Klimas, A. J., Valdivia, J. A., Vassiliadis, D., Baker, D. N., Hesse, M., and Takalo, J.: Self-organized criticality in the substorm phenomenon and its relation to localized reconnection in the magnetospheric plasma sheet, J. Geophys. Res., 105, 18 765, 2000.

Landau, L. and Lifshitz, E. M.: Statisticheskaja Fizika, Moskva, Nauka, 1976.

Lewis, Z. V.: On the apparent randomness of substorm onset, Geophys. Res. Lett., 18, 1627, 1991.

Lorenz, E. N.: Determining nonperiodic flow, J. Atmos. Sci., 20, 130, 1963.

Lu, E. T.: Avalanches in continuum dissipative systems, Phys. Rev. Lett., 74, 2511, 1995.

Mackey, M. C. and Glass, L.: Oscillation and chaos in physiological control systems, Science, 197, 287, 1977.

Mead, W. C., Jones, R. D., Lee, Y. C., Barnes, C. W., Flake, G. W., Lee, L. A., and O'Rourke, M. K.: Prediction of chaotic time series using CNLS-net-example: The Mackey-Glass equation, in: Nonlinear Modeling and Forecasting, Santa Fe Institute Studies in the Science of Complexity XV, edited by Casdagli, M., and Eubank, S., Addison-Wesley, 1992.

Meyer, T. P. and Packard, N. H.: Local forecasting of high dimensional chaotic dynamics, in: Nonlinear Modeling and Forecasting, Santa Fe Institute Studies in the Science of Complexity XV, edited by Casdagli, M., and Eubank, S., Addison-Wesley, 1992.

Muldoon, M. R., Broomhead, D. S., Huke, J. P., and Delay, R. H.: Embedding in the presence of dynamical noise, Dynamics and Stability of Systems, 13, 175, 1998.

Nagai, T., Fujimoto, M., Saito, Y., Mashida, S., Terasawa, T., Nakamura, R., Yamamoto, T., Mukai, T., Nishida, A., and Kokubun, S.: Structure and dynamnics of magnetic reconnection for substorm onsets with Geotail observations, J. Geohys. Res. 103, 4419, 1998.

Ohtani, S., Higuchi, T., Lui, A. T., and Takahashi, K.: Magnetic fluctuations associated with tail current disruption: Fractal analysis, J. Geophys. Res., 100, 19 135, 1995.

Pecora, L. M. and Carroll, T. L.: Synchronization in chaotic systems, Phys. Rev. Lett., 64, 821, 1990.

Petrukovich, A. A., Sergeev, V. A., Zelenyi, L. M., Mukai, T., Yamamoto, T., Kokubun, S., Shiokawa, K., Deehr, C. S., Budnick, E. Y., Buchner, J., Fedorov, A. O., Grigorieva, V. P., Hughes, T. J., Pissarenko, N. F., Romanov, S. A., and Sandhal, I.: Two spacecraft observations of a reconnection pulse during an auroral breakup, J. Geophys. Res., 103, 47, 1998.

Price, C. P., Prichard, D., and Bischoff, J. E.: Nonlinear input/output analysis of the auroral electrojet index, J. Geophys. Res., 99, 13 227, 1994.

Prichard, D. and Price, C. P.: Is the AE index the result of nonlinear dynamics?, Geophys. Res. Lett., 20(24), 2817, 1992.

Rhodes, C. and Morari, M.: Determening the model order of nonlinear input/output systems, IfA Technical Report AUT97-01, Automatic Control Lab -ETH Zurich, 1997.

Sauer, T., Yorke, J. A., and Casdagli, M.: Embedology, J. Stat. Phys., 65, 579, 1991.

Sauer, T.: Time series prediction by using delay coordinate embedding, in: Time Series Prediction: Forecasting the Future and Understanding the Past, Santa Fe Institute Studies in the Science of Complexity XV, edited by Weigend, A. S. and Gershenfeld, N. A., Addison-Wesley, Reading, MA, 1993.

Sharma, A. S.: Assessing the magnetosphere's nonlinear behavior: Its dimension is low, its predictability high (US National Report to IUGG, 1991–1994), Rev. Geophys. Supple., 33, 645–650, 1995.

Sharma, A. S., Vassiliadis, D., and Papadopoulos, K.: Reconstruc-

tion of low dimensional magnetospheric dynamics by singular spectrum analysis, Geophys. Res. Lett., 20, 335, 1993.

Sharma, A. S., Sitnov, M. I., and Papadopoulos, K.: Substorms as nonequilibrium transitions in the magnetosphere, J. Atmos. Solar Terrest. Physics, 63, 1399, 2001.

Sitnov, M. I., Sharma, A. S., Papadopoulos, K., Vassiliadis, D., Valdivia, J. A., Klimas, A. J., and Baker, D. N.: Phase transition-like behavior of the magnetosphere during substorms, J. Geophys. Res., 105, 12 955, 2000.

Sitnov, M. I., Sharma, A. S., Papadopoulos, K., and Vassiliadis, D.: Modeling substorm dynamics of the magnetosphere: From self-organization and self-criticality to nonequilibrium phase transitions, Phys. Rev. E., 65, 01611-6, 2001.

Stanley, H. E.: Introduction to Phase Transition and Critical Phenomena, Oxford Univ. Press, New York, 1971.

Stark, J., Broomhead, D. S., Davis, M. E., and Huke, J.: Takens embedding theorems for forced and stochastic systems, Second World Congress of Nonlinear Analysis, 1996.

Stark, J.: Delay reconstruction: dynamics versus statistics, Nonlinear Dynamics and Statistics, A.I. Mees, Birkhauser, 2001.

Takalo, J., Timonen, J., Klimas, A. J., Valdivia, J. A., and Vassiliadis, D.: Nonlinear energy dissipation in a cellular automation magnetotail model, Geophys. Res. Lett, 26, 1813, 1999.

Takalo, J., Timonen, J., and Koskinen, H.: Correlation dimension and affinity of AE data and bicolored noise, Geophys. Res. Lett., 20, 1527, 1993.

Takalo, J., Timonen, J., and Koskinen, H.: Properties of AE data and bicolored noise, J. Geophys. Res., 99, 13 239, 1994.

Takens, F.: Detecting strange attractors in fluid turbulence, in: Dynamical Systems and Turbulence, edited by Rand, D. and Young, L. S., Springer, Berlin, 1981.

Theiler, J.: Some comments on the correlation dimension of $1/f^{\alpha}$ noise, Phys. Lett. A, 155, 480, 1991.

Tsurutani, B. T., Sugiura, M., Iyemori, T., Goldstein, B. E., Gonzalez, W. D., Akasofu, S. I., and Smith, E. J.: The nonlinear response of AE to the IMF Bs driver: A spectral break at 5 hours, Geophys. Res. Lett., 17, 279, 1990.

Ukhorskiy, A. Y., Sitnov, M. I., Sharma, A. S., and Papadopoulos, K.: Global and multi-scale properties of magnetospheric dynamics in local-linear filter, J. Geophys. Res. 107(A11), 1369, 2002a.

Ukhorskiy, A. Y., Sitnov, M. I., Sharma, A. S., and Papadopoulos, K.: Proceedings of the 6th International Conference on Substorms, Seattle, Washington, USA, March 25-29, 2002b.

Uritsky, V. M. and Pudovkin, M. I.: Low frequency $1/f$-like fluctuations of the AE-index as a possible manifestation of self-organized criticality in the magnetosphere, Ann. Geophysicae, 16(12), 1580, 1998.

Uritsky, V., Klimas, A. J., Vassiliadis, D., Chua, D., and Parks, G.: Scale-free statistics of spatiotemporal auroral emissions as depicted by PLAR UVI images: Dynamic magnetosphere is an avalanching system, J. Geophys. Res., 107, 1426, doi: 10.1029/2001JA000281, 2002.

Valdivia, J. A., Sharma, A. S., and Papadopoulos, K.: Prediction of magnetic storms by nonlinear models, Geophys. Res. Lett., 23, 2899, 1996.

Vassiliadis, D., Klimas, A. J., Baker, D. B., and Roberts, D. A.: A description of the solar wind-magnetosphere coupling based on nonlinear filters, J. Geophys. Res., 100, 3495, 1995.

Vassiliadis, D., Sharma, A. S., Eastman, T. E., and Papadopoulos, K.: Low dimensional chaos in magnetospheric activity from AE time series, Geophys. Res. Lett., 17, 1841, 1990.

Vespignani, A. and Zapperi, S.: How self-organized criticality works: A unified mean-field picture, Phys. Rev. E, 57, 6345, 1998.

Watkins, N. W., Freeman, M. P., Chapman, S. C., and Deny, R. O.: Testing the SOC hypothesis for the magnetosphere, JASTP, 63, 1435, 2001.

Watkins, N. W., Chapman, S. C., Dendy, R. O., and Rowlands, G.: Robustness of collective behaviour in strongly driven avalanche models: magnetospheric implications, Geophys. Res. Lett., 26, 2617, 1999.

Weigel, R. S., Vassiliadis, D., and Klimas, A. J.: Coupling of the solar wind to temporal fluctuations in ground magnetic fields, Geophys. Res. Lett., 29, 10.1029/2002GL014740, 2002.

Zheng, B., Schulz, M., and Trimper, S.: Deterministic equations of motion and dynamic critical phenomena, Phys. Rev. Lett., 82, 1891, 1999.